Modeling of Metal-plate-connected Wood Truss Joints

M. Vatovec, T. H. Miller, R. Gupta

Abstract. *A commercially available, three-dimensional finite-element analysis software was used to model the load-displacement behavior of metal-plate-connected (MPC) joints in wooden trusses. Model features included consideration of material properties, teeth-to-grain-to-direction-of-force orientation, wood-to-wood interaction, and gaps between wood members. To simulate wood-to-plate interaction, the main feature of the model, each tooth of the metal plate is represented by one set of three spring elements. Each spring element accounts for tooth-wood behavior (stiffness) in one major plate direction: parallel to slots, perpendicular to slots in the plane of the plate, and perpendicular to the plane of the plate. For each element, nonlinear load-slip (stiffness) curves are defined based on tension splice joint tests at various teeth-to-grain orientations. One advantage of the spring-element-based approach is that once incorporated in the model, the per-tooth stiffness need not be adjusted for different loading conditions applied later to the joint model.*

The load-displacement (L-D) results from the model compared very well to the experimental results from tensile and bending tests of splice joints with several different teeth-to-grain orientations. For the investigated plate size, the governing factor for joint behavior was the plate-wood interaction (spring elements). Several possible model simplifications were investigated. Models with lumped teeth properties predict joint L-D behavior reasonably well.
Keywords. *Wood engineering, Trusses, Joints, Metal-plate-connectors, Modeling.*

The behavior of metal-plate-connected (MPC) joints in service is complex and difficult to analyze without experimental data and validation. Better analyses of joints contribute to an understanding of the overall behavior of MPC trusses, and could lead to improvements in current design practices, and in turn improved cost effectiveness and safety of engineered trusses.

To date, one of the most advanced methods for determining properties of MPC joints was a model developed by Foschi (1979), who used a three-parameter equation to characterize the nonlinear load-slip behavior of connections. The basic load-slip properties associated with the entire wood-member areas covered by the plate are determined from the four tests defined by the Canadian Standards Association (1980). Foschi's connector model was implemented in a computer program Structural Analysis of Trusses (SAT) (Foschi, 1979).

Triche and Suddarth (1988) developed a new program (PPSAFT) by modifying and extending the SAT program so that it would provide design information for the lumber members as well as for the plate connectors. Cramer et al. (1993) presented an alternate stiffness-calculation method in the SAT model, as well as developed automated means to compute the geometric characteristics of each plate-wood contact surface.

Earlier, Cramer et al. (1990) presented a nonlinear, plane-stress finite-element model that allows computation of the internal deformations, stress conditions, and ultimate strength for MPC joints loaded in tension and bending. Reynolds (1988) expanded an existing finite-element analysis program by adding the "interface element" (linear, two-dimensional triangular elements with zero thickness) stiffness matrix to account for the overall wood-plate interface behavior. Crovella and Gebremedhin (1990) developed an elastic foundation model (based on the assumption that each tooth acts as a cantilever beam in an elastic supporting medium) and a simple finite-element model to predict joint stiffness.

Although some of the existing models incorporate many elements of MPC truss joint behavior, most require additional calculation adjustments depending on loading conditions (direction of forces applied to joints with respect to wood and grain orientations). Furthermore, most of these models do not use commercially available software to model MPC joints.

The main objective of this study was to develop and test a three-dimensional, finite-element model that would accurately represent wood-truss MPC joints and their behavior in service, and provide comprehensive information on the displacements of joints and forces in joint members when loaded. The model will be able to incorporate the major factors that influence the performance of MPC joints: wood and steel properties, load-slip relationship between steel plates and wood members depending on plate-to-grain-orientation, wood-to-

Article was submitted for publication in September 1995; reviewed and approved for publication by the Structures and Environment Div. of ASAE in March 1996. Presented as ASAE Paper No. 95-4586.

Research supported by the Center for Wood Utilization Research Grants (USDA Special Grant), Department of Forest Products, College of Forestry, Oregon State University, Corvallis.

The authors are **Milan Vatovec**, Faculty Research Assistant, Dept. of Forest Products, **Thomas H. Miller**, Assistant Professor, Dept. of Civil Engineering, and **Rakesh Gupta**, ***ASAE Member Engineer,*** Assistant Professor, Dept. of Forest Products, Oregon State University, Corvallis. **Corresponding author:** Milan Vatovec, Dept. of Forest Products, Oregon State University, Corvallis, OR 97331; telephone: 503-737-4243; fax: 503-737-3385; e-mail: <vatovecm@frl.orst.edu>.

wood contact, and eccentricity and gaps between wood members.

A further goal of this project was to establish basic principles and methodology for developing a simplified version of the model discussed here, by investigating the load-displacement results, and evaluating the importance of model input parameters. This new model will be more readily applicable to design, while still providing a high level of accuracy in predicting MPC joint/truss behavior.

The process of developing the model consisted of several steps. We first constructed a finite-element model of MPC joints capable of representing joint behavior under various loading conditions. We then conducted several series of tensile tests on MPC joints to obtain input parameters and to evaluate the model performance (some of the joints used to obtain input parameters were modeled and the results were compared). The model was further investigated for sensitivity to various input parameters, then re-evaluated through comparisons with the results of additional tensile and bending MPC-joint tests. After final validation of the model, we considered possible model simplifications.

METHODS

DEVELOPMENT OF FINITE-ELEMENT MODEL FOR MPC JOINTS

All joint modeling was accomplished with a commercial software, ANSYS® (1992), a general-purpose, finite-element analysis program. We used ANSYS because it is a powerful tool capable of, but not limited to, performing the analysis of individual MPC joints; it will allow for more extensive design and optimization analyses of MPC joints and full-scale trusses in the future; and, it is widely available.

Our basic approach was to build a finite-element model to represent the joint behavior "from the bottom up" by first incorporating the parameters influencing the joint behavior at the per-tooth level, then building the rest of the model and exposing it to a particular set of global boundary and static loading conditions.

All joints were modeled in three dimensions. Since one of our major goals was to represent MPC joints in the most realistic manner possible, we selected ANSYS element types capable of including most parameters describing the physical and mechanical properties of the constituent materials, as well as the parameters associated with interaction of the components (plate and wood).

Wood and Steel-plate Elements. A simplified schematic of a portion of a typical MPC joint, along with the approach used to model it, are shown in figures 1a and 1b, respectively. The wood members and steel plates of the MPC joints were modeled with the *3-D Structural Solid* elements (ANSYS element 45, ANSYS, 1992), and are shown in figure 1b. Each element consisted of eight nodes. Wood and plate elements were defined by two independent sets of nodes, some of them geometrically coincident (along the plane between the plate and wood). The mesh of elements preserved the actual global geometry of the joint, although only one quarter of the joint was modeled. This was possible since all modeled MPC joints were symmetric with respect to the plane parallel to and between the plates, and to the plane coinciding with the wood member-to-

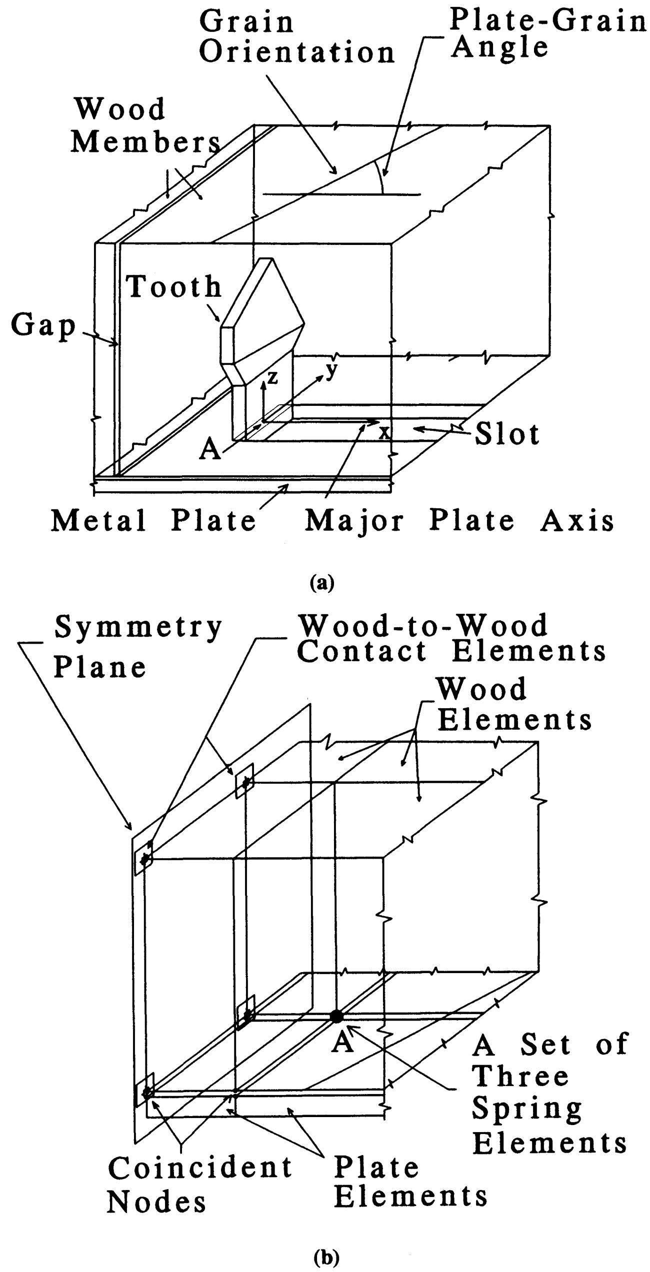

Figure 1–(a) Simplified schematic of a typical MPC joint: wood members, plate, plate-grain orientation, and (b) simplified schematic of a joint model: wood and plate elements, spring elements representing wood-plate interaction, and wood-to-wood elements.

member interface plane. A set of boundary conditions was then imposed, preventing the nodes on those two planes from rotating about the two axes defining the planes of symmetry, as well as translating in the direction perpendicular to the planes of symmetry.

The metal plates used for fabrication of joints were supplied by Alpine Engineered Products®, Pompano Beach, Florida. Properties of plates and steel coils (from which the plates were manufactured) are shown in table 1. The steel plate elements in the model were assigned elastic-plastic bilinear material properties (modulus of elasticity and yield point) as shown in the table.

The material properties for the wood portion of the model include moduli of elasticity (MOE) in the three

Table 1. Metal plate specifications, test results, and dimensions

Plate Description	Plate Specifications and Dimensions
Type of steel	ASTM A446 Grade A, with ASTM A525 G60 coating
Modulus of elasticity	200 000 MPa
Average yield strength	327 MPa (47.4 ksi)
Average ultimate strength	357 MPa (51.8 ksi)
Plate net thickness	0.876 mm (20 gauge)
Tooth net length	8.4 mm (0.33 in)
Slots dimensions	12.2 × 3.2 mm (0.5 × 0.125 in.) in-line
Tooth density	1.24 teeth per 100 mm^2 (8 teeth per $in.^2$)
Teeth configuration	In-line and twisted
Dimensions of tested plates	76 × 102 mm (3 × 4 in.) and 25 × 76 mm (1 × 3 in.)

principal orientations (longitudinal, radial, and tangential). The longitudinal MOE values for each model were assigned based on the corresponding average test values (table 2), and the MOE properties for the other two orientations were derived from the longitudinal MOE values with the guidelines given in the Wood Handbook (Forest Products Laboratory, 1987).

Spring Elements. The interaction between wood members and steel plate teeth in the finite-element model was represented by *Nonlinear Spring* elements (ANSYS element 39). The spring elements in the model assume the "role" of the tooth on the plate. This feature, and the way it is incorporated in the model, is probably the most important component of the model. The spring elements define the plate-to-grain-orientation-dependent load-slip relationships (stiffnesses) for the joint on a per-tooth level, and govern the overall behavior of the joint.

Table 2. Test results—average test L-D curve parameters, S.G., and MOE data

	No. of Obs.		m_0 (N)	k (N/mm)	m_1 (N/mm)	S.G.	MOE (MPa)
T0	6	Mean	231	1380	94	0.56	15 800
		COV	0.07	0.18	20.40	0.14	0.11
T30	5	Mean	197	937	42	0.53	13 600
		COV	0.22	0.27	0.87	0.12	0.16
T60	6	Mean	166	865	49	0.51	13 100
		COV	0.10	0.17	0.35	0.14	0.18
T90	6	Mean	338	261	−82	0.55	14 100
		COV	0.30	0.16	0.73	0.08	0.11
TP0	6	Mean	645	350	−181	0.56	15 100
		COV	0.84	0.18	1.19	0.12	0.13
TP30	5	Mean	158	853	40	0.52	13 600
		COV	0.46	0.22	1.82	0.12	0.16
TP60	5	Mean	167	1190	42	0.50	12 500
		COV	0.12	0.07	0.40	0.12	0.16
TP90	6	Mean	202	1310	21	0.55	14 800
		COV	0.26	0.21	1.40	0.11	0.12
R30	5	Mean	207	1040	44	0.58	16 100
		COV	0.05	0.07	0.18	0.10	0.12
R60	6	Mean	212	1010	27	0.55	14 600
		COV	0.08	0.10	0.34	0.10	0.15
B0	5	Mean	12 700	1560	−195	0.50	14 200
*		COV	0.27	0.11	0.98	0.09	0.13
B30	5	Mean	11 700	1240	−156	0.50	14 000
*		COV	0.47	0.17	1.54	0.09	0.12
B60	5	Mean	7390	1790	−40	0.52	15 700
*		COV	0.42	0.17	4.64	0.10	0.13
B90	5	Mean	15 300	1470	−462	0.54	14 700
*		COV	0.86	0.24	1.50	0.13	0.11

* Test results shown are not on a per-tooth basis.

Although we attempted to preserve the actual joint geometry in the modeling process, we needed to make some assumptions and simplifications. The steel plate was modeled without slots between the teeth, and the three-dimensional nature of the teeth was modeled as wood-teeth interaction that occurs at one, nondimensional point, as shown in figure 1b (point A). The complex nature of the force-carrying mechanism of each tooth was difficult to characterize, and it significantly complicated the model in early attempts where all teeth had been modeled in three dimensions. We therefore characterized the teeth behavior by "lumping" the tooth action at one, nondimensional point. By doing so, a compromise was made with respect to the stresses created in the wood member (in the vicinity of the plate) and in the plate, yet it was assumed that most other model output parameters remained unaffected.

It is important to emphasize that although we did not model the teeth in three dimensions, we retained the three-dimensional approach for modeling the joints, in order to correctly represent the eccentric load-carrying mechanism in the connections (the overlap of the metal plates and wood members).

Thus, the load-slip characteristics of each tooth with respect to wood were represented by a set of three non-linear spring elements "connecting" two coincident nodes in the model, one belonging to wood, the other to the plate. Each spring element was defined by a single load-displacement (L-D) curve, defined by the user, which was input to represent the per-tooth load-slip behavior (stiffness) in one of the three principal plate orientations. The three principal plate (teeth) orientations were recognized as the major plate axis (x) that coincides with the direction of the plate slots, the minor plate axis (y) that is in the plane of the plate, but perpendicular to x, and the z axis that is perpendicular to the plate (fig. 1a).

The finite-element model's L-D parameters characterizing the behavior (stiffness) of spring elements in the plane of the plate (x and y directions) were ascertained through tensile tests on simple joints, which eliminated the need for more expensive procedures involving testing of various joint configurations. These tensile tests were unique for one plate-to-grain orientation (and in general for a particular wood species, plate type, etc.). The properties of spring elements characterizing wood-plate interaction in the direction perpendicular to the plate (z-direction) were obtained from a pilot study (Vatovec, 1996).

Contact Elements. When MPC joints are loaded in compression or bending, or are subject to eccentric axial loading, the overall behavior of the joint is greatly influenced by the wood surfaces that come into contact. Therefore, the presence of contact elements in the model is essential. The size of the gap that is created between the real joint members during fabrication governs the occurrence of contact.

Wood-to-wood interaction in the MPC joints was represented by the *3-D Point-to-Point Contact Elements* (ANSYS, element 52), shown in figure 1b. The contact element represents two surfaces that may maintain or break physical contact and may slide relative to each other. The contact elements are capable of supporting only compression in the direction normal to the surfaces that come in contact, and shear (Coulomb friction) in the tangential direction. In the model, they were used to represent the physical interaction of two or more wood members that may come into contact while the joint is loaded. If the surfaces do not touch, the contact elements do not influence the behavior of the model. Physically, they connect two geometrically noncoincident nodes, each belonging to one of the wood members that may come into contact.

Since only one quarter of each joint was modeled (only one half of one wood member), the contact elements were placed to connect each wood node that would ordinarily touch the other wood member when loaded in bending, with another node from a set of properly constrained nodes located in the plane of wood-to-wood interaction. These nodes were used in the model solely for the purpose of constraining joints loaded in bending (assuming the role of the other wood member), and were prevented from translation in all directions except in the direction of applied load.

The properties of contact elements were assigned according to the recommendations given by ANSYS (ANSYS, 1992). Each contact element was defined by two stiffnesses—the Coulomb coefficient of friction (0.4) for wood-to-wood contact governing stiffness properties in the plane of contact (Eshbach, 1990); and stiffness in the direction perpendicular to the plane of contact (87 $N/mm/mm^2$), estimated as an order of magnitude greater than the adjacent wood element's stiffness, as recommended by the ANSYS program guidelines. The stiffness value for the adjacent wood elements was validated by a set of compression tests on small clear wood specimens (Vatovec, 1995).

Fabrication of MPC Joints

Lumber used in this study was machine-stress-rated (MSR 1800f 1.6E) nominal 2 × 4 in. (38 × 89 mm) and nominal 2 × 6 in. (38 × 140 mm) Douglas-Fir lumber from Frank Lumber Co., Mill City, Oregon, with an MOE of at least 11 000 MPa (1.6 million psi). The MOE and specific gravity (SG) of each board were determined before the lumber was conditioned in a controlled environment at 20°C, and 70% RH (relative humidity).

As mentioned before, metal plates used for fabrication of joints were supplied by Alpine Engineered Products, Pompano Beach, Florida.

The MPC joints were fabricated as shown in figures 2 and 3.

Testing of MPC Joints

We tested MPC joints both to obtain model input parameters and to validate the model as it was developed in this study. Tensile tests were conducted to determine input parameters; tensile and bending tests were used to validate the model.

Six MPC joint specimens were tested for each specific test configuration (84 joints total). Within each test configuration, specimens were cut out of six different pieces of lumber. Some data were discarded due to fixture failures and failures at locations other than near the plates. Testing of all joints was implemented with a constant-rate-of-displacement, 36 000 N (8,000 lb) capacity universal testing machine. The testing rate was 1 mm/min. All joint specimens were loaded until failure.

Tests to Determine Model Parameters. We conducted tensile tests to obtain teeth load-slip parameters (stiffnesses) in the direction parallel to the major axis of the plate (parallel to plate slots), which we refer to as T tests (fig. 2a), and in the direction perpendicular to the plate major axis (perpendicular to plate slots), which we refer to as TP tests (fig. 2b). For both types of tests, the orientations of wood grain to the major axis of the plate were 0, 30, 60, and 90°, and the load was applied either parallel (T tests), or perpendicular (TP tests) to the plate major axis. The T and TP test configurations, and the specimen dimensions, are shown in figures 2a and 2b. The numbers following the letters designate the angle in degrees between the direction of the grain and the plate major axis.

The geometric constraints associated with nominal 2 × 6 in. boards, in fabrication of joints where the plate-grain orientation was 30° (T30 and TP30) and 60° (T60 and TP60), resulted in specimens with maximum lengths of 126 and 110 mm, respectively (after cutting the specimens out of boards at appropriate grain angles). In order to preserve a sufficient overall length for the specimens (to enable positioning of displacement transducers), the joints were fabricated such that only one member had the desired plate-grain orientation, while the other member was longer, with the grain oriented parallel to the long member edge. For these reasons, in all tensile tests, the area covered with the plate was clamped on one side of the joint (the longer member side), therefore preventing displacements and failure of the plate or wood on that side. Hence, the behavior of only one half of each joint was investigated.

The grain-angle associated geometric constraints, along with the fact that specimens tend to split along the grain at higher loads instead of failing at the joint if a full-size plate is used, in turn prompted the use of smaller plates in the T30, T60, TP30, and TP60 tests. In order to justify the use of smaller plates (validate the assumption that the stiffnesses of all the teeth in the plate are approximately equal), an extra set of tensile tests was conducted with T0 plate-grain orientation, but with a smaller plate size [25 × 76 mm (1 × 3 in.)]. The average per-tooth L-D curves were obtained by dividing the load values by the appropriate number of teeth for corresponding tests. After observing that there was no significant difference between the average per-tooth L-D curves for those two joint configurations, we concluded that smaller plates could be used to determine per-tooth load-slip characteristics for intermediate plate-to-grain orientations.

Two displacement transducers (linear variable differential transducers, or LVDTs) were used to measure displacements of the "investigated" side of the joint relative to the clamped side. The LVDTs were attached to the wood member 25 mm above the metal plate to measure displacements relative to the plane between the two members. Force and the average axial displacement were continually recorded and saved via a data acquisition system in a computer file.

Tests to obtain the load-displacement properties for the direction perpendicular to the plate (plate stiffness in withdrawal) were not implemented in this study, and the L-D data were obtained from a pilot study (Vatovec, 1996).

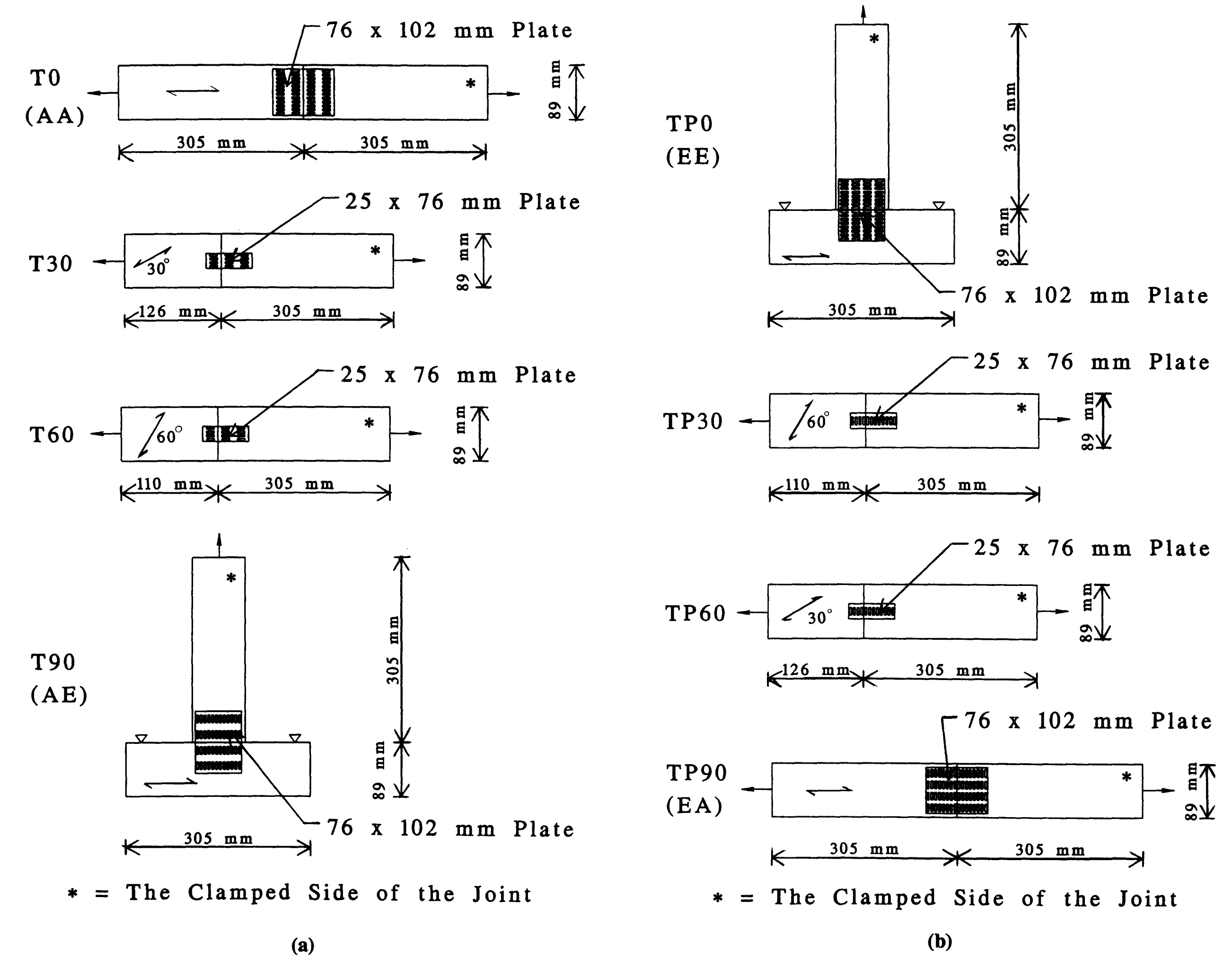

Figure 2–Test configurations where load was applied parallel to the main plate axis (T tests) and where load was applied perpendicular to the plate main axis (TP tests), for various plate-grain orientations (0, 30, 60, and 90°). (a) T tests and (b) TP tests. The symbols in parentheses designate the customary notation, defined by Foschi (1979).

Tests to Validate the Model. Two different types of tests were conducted to validate the model: tensile (R) tests, and bending (B) tests (figs. 3a and 3b, respectively). The overall L-D behaviors of these test specimens were compared to those obtained from the model.

The seemingly simple configurations of these joints (tensile and bending joints with various plate-grain orientations) exemplify the conditions existing in a variety of typical truss-joint configurations when in service. Separate wood truss members in actual truss joints can be oriented at any angle to the plate major axis and can be exposed to a variety of different loads when in service. To validate the model, we chose joints that represented situations typically existing in actual truss joints (various plate-grain, and plate-grain-load orientations). Two different joint configurations were tested in tension (R30 and R60). In both cases the force was applied parallel to the grain, through the axial centroid of the joints. However, the plate-to-grain orientation was varied (30 and 60°). Figure 3a summarizes these two joint configurations. The plate dimensions were 76 × 102 mm, but they were cut such that the plate major axis was not parallel to either edge of the plate. The test setup was identical to the setup for T0 and TP90 tests.

Four joint configurations were tested in bending. The angle between wood grain and plate major axis was varied, while keeping the plate size constant. Four different plate-grain angle combinations were tested: 0, 30, 60, and 90° (B0, B30, B60, and B90). Bending specimens and the dimensions are shown in figure 3b.

Bending specimens were tested on a span of 760 mm, and the load was applied at one-third points. The load and the mid-span vertical deflection (measured at the center of the plate) were continually monitored until failure.

Test Data Analyses. Load-displacement curves for all joints were recorded and plotted. For all tests, the observed deflection was associated with the direction of the applied load. For each tensile test, the load values were divided by the number of teeth in the half of the joint of interest to obtain the per-tooth L-D curves. To simplify the process of assigning model properties, we assumed that all teeth over the entire area of the plate had approximately the same stiffness (Foschi, 1979).

A computer-based, nonlinear curve-fitting technique was used to fit a three-parameter equation to each specimen data set. The well-known and accepted Foschi (1979) equation was found to fit the data quite well.

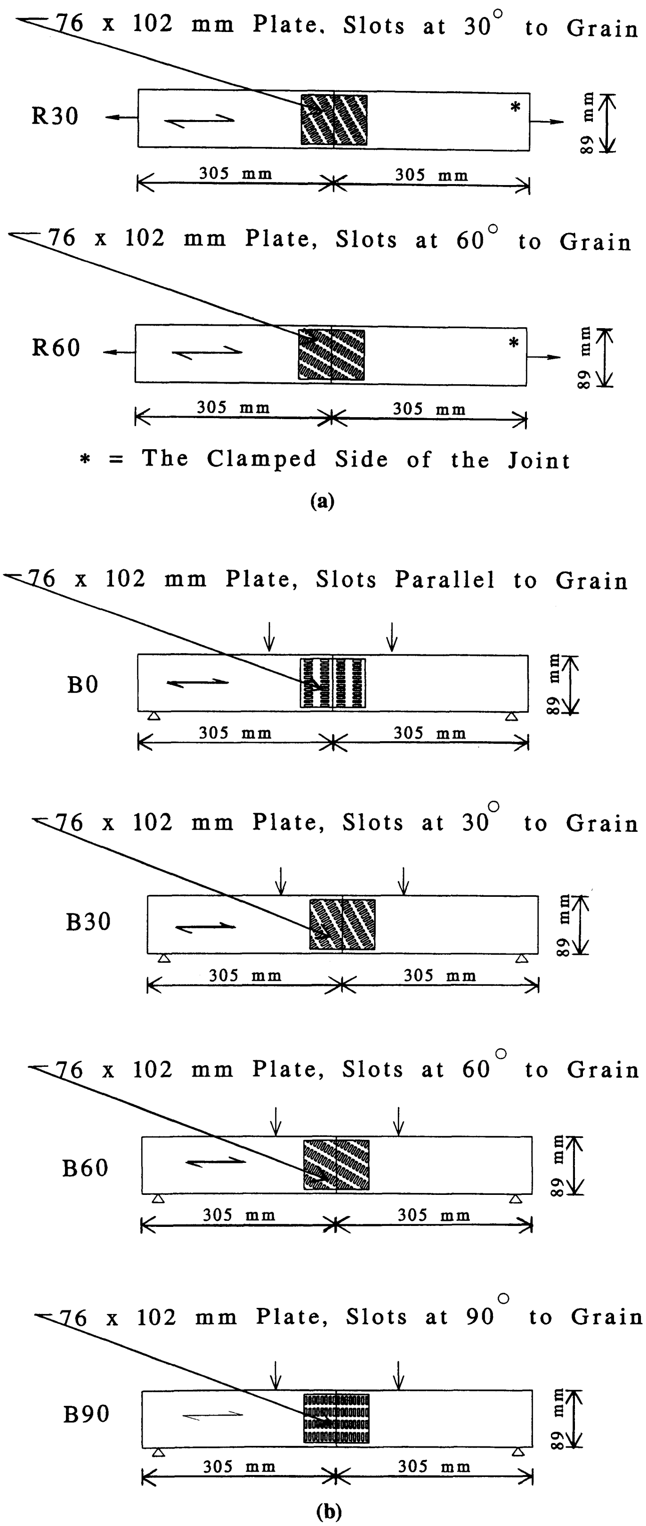

Figure 3–Tensile test configurations where load was applied parallel to the grain orientation (R tests) and bending test configurations where load was applied at third span perpendicular to the grain orientation (B tests), for various plate-grain orientations. (a) R tests (plate-grain orientation at 30 and 60°), and (b) B tests (plate-grain orientation at 0, 30, 60, and 90°).

$$F = (m_0 + m_1 |\Delta|)\,[1 - \exp(-k|\Delta|/m_0)] \qquad (1)$$

where F represents load, Δ represents displacement, and k, m_1, and m_0 are equation parameters, representing the L-D curves' initial slope (initial stiffness), the slope of the asymptote at large deflections (stiffness at large slip), and the y-axis intercept of the asymptote with slope m_1, respectively.

The average values for each of the equation parameters (k, m_0, and m_1) were found for each group of six tests, and are shown in table 2 (on a per-tooth basis for tensile tests). According to the method presented by McCarthy and Wolfe (1987), we used those average parameter values to define the average test curves, which were then used to represent the behavior of specific tested joints in later analysis.

Model Parameters

The average per-tooth L-D curves for T and TP tests are shown in figures 4a and 4b, respectively. Note that in both cases the curves for intermediate angles (30, 60°) fall in the region between the two basic curves, as expected. The order is reversed for the tests where the load was oriented perpendicular to the plate's major direction, which agrees with McCarthy and Wolfe (1987), and may be attributed to the stiffer response of joints when force is applied parallel (or close to parallel) to the direction of the grain.

The method of assigning in-plane stiffness properties to spring elements in particular models is shown in figure 5.

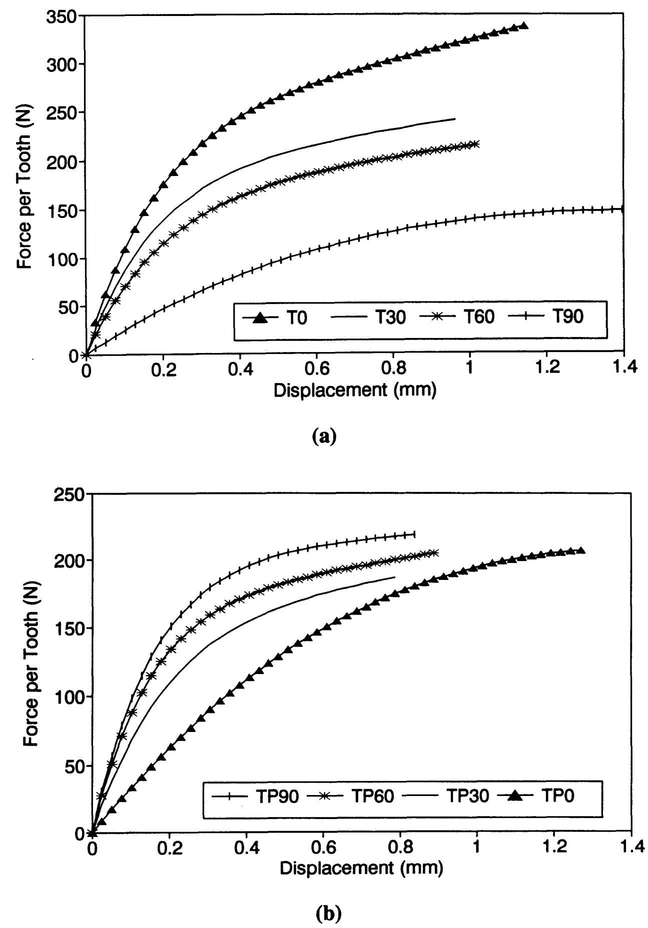

Figure 4–Average per-tooth load-displacement curves for tests with plate-grain orientation at 0, 30, 60, and 90°, where load was applied (a) parallel to the plate main axis, (T0, T30, T60, and T90 tests), and (b) perpendicular to the plate main axis, (TP0, TP30, TP60, and TP90 tests).

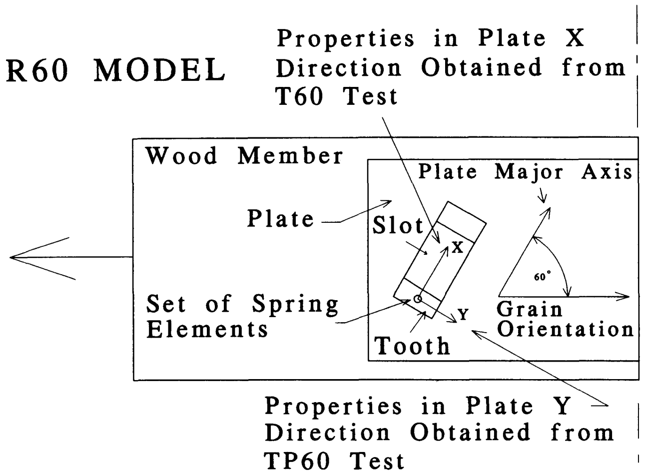

Figure 5–Schematic for a model where load is applied parallel to the grain and the plate is oriented at 60° with respect to the grain (R60 model): orientation of assigned load-slip properties.

For instance, in order to model a joint where the angle between the plate major orientation (x axis) and grain is 60° (models R60 and B60), one needs to obtain the per-tooth load-slip (stiffness) characteristics in the x and y plate directions from only two tensile tests. The per-tooth stiffness properties in the direction parallel to the plate major axis will be determined from the T60 tests, since for that test the angle between the plate major axis and grain is 60°, and the force is applied along the plate x axis. Similarly, the stiffness properties in the direction perpendicular to the plate main axis (y direction) were determined from the TP60 tests, where the plate-grain orientation was again 60°, and the force was applied along the y axis. Once the assigned per-tooth load-slip characteristics (stiffnesses) are incorporated to the model, they need not be adjusted for different load conditions (orientations, magnitudes, etc.) applied later to the joint model. Table 3 shows the appropriate tests used to determine the per-tooth stiffness characteristics in the x and y directions for all models developed in this study.

The per-tooth load-slip behavior of plates in withdrawal was assumed independent of plate-to-grain orientation, and the average curve from a pilot test (Vatovec, 1996) was used to characterize the joint load-slip behavior in the z direction for all models created in this study.

The ANSYS program does not generate a per-tooth stiffness curve directly from the three L-D equation parameters input by the user. Each spring element is defined by a set of discrete L-D points. Therefore, from each of the average L-D curves (from T and TP tests), characterizing a per-tooth stiffness for a particular plate-to-grain orientation, a set of discrete points along the plotted line was visually selected to best "describe" the nature of the curve.

Table 3. Tests used to obtain model parameters

Model	Test to Determine Properties in the Plate x Direction	Test to Determine Properties in the Plate y Direction
T0, TP0, B0	T0	TP0
T90, TP90, B90	T90	TP90
R30, B30	T30	TP30
R60, B60	T60	TP60

Validation of Four Basic Tensile Models and Sensitivity Analysis

Validation of Four Basic Tensile Models. The first models developed in this study actually represented basic joint geometries, under simple load configurations. Specifically, we developed a model for each of the basic four tests described by the Canadian Standard (1980) (in this text identified as T0, T90, TP0, and TP90), for the purpose of comparing them to model outputs.

All models copied the geometry and simulated the loading conditions of the corresponding physical tests. The loads in the models were applied in a number of discrete load steps, with the final load step magnitude near the average failure load for the corresponding physical test.

Sensitivity Analysis. Before proceeding to compare the model performance against the physical tests where the influence of plate-grain orientation was investigated (R and B tests), we performed a sensitivity analysis to determine which parameters govern the behavior of the T0 joint model. The influences of several model input parameters on the overall joint stiffness were investigated: the assigned wood member and steel element stiffnesses, and the assigned per-tooth load-slip parameters in the plane of the plate and perpendicular to the plane of the plate (z-direction).

Model Validation

Models were developed for each of the R and B joint configurations for the purpose of comparing the model L-D output to the joint testing results.

R Models. The element layout and loading conditions for models representing R30 and R60 joints simulated the actual conditions of the corresponding physical tests. The geometric pattern of the nodes defining the location of spring element sets (original teeth locations) coincided with the teeth pattern of the tested joint. The forces in these two models (R30 and R60) were not coincident with the direction of either plate axis.

The average per-tooth L-D testing curves for R30 and R60 tests were converted into full joint L-D curves by adjusting for the number of teeth in the appropriate models, and were compared to the appropriate model outputs.

B Models. The models representing MPC joints loaded in bending were based on the same nodal geometry used for the corresponding tensile models (T0, R30, R60, and TP90). The differences were in the loading and boundary conditions (third-span point loading, and the reaction point node prevented from translation). Also, a number of wood-to-wood contact elements were inserted along the wood surfaces that came into contact during bending.

Model Simplifications

In this study, we aimed at developing a comprehensive model of MPC joints capable of realistically representing the behavior and characteristics of actual joint configurations. However, in an attempt to reduce the overall analysis time involved in the model creation process, and perhaps enable this concept to become more useful to the truss industry, several possible model simplifications, along with some simplifications already incorporated in the model, were examined. We developed several models to address specific simplifications for the purpose of comparing their output to the joint test results.

Plate Slots. Initially, modeling of the joints included the slots in the metal plate. This process complicated the analysis significantly, and we attempted to eliminate the slots. All metal plates were modeled without taking the slots between the teeth into consideration. All steel plates were considered rectangular in shape, with thickness being the actual thickness of the plate. To investigate the influence of plate slots on the overall model's L-D behavior, the outputs of T0 models developed with and without slots were compared.

Teeth Layout. The geometric layout for wood-to-steel elements in the R30 and R60 models copied the actual teeth pattern in real joints. The area beneath the plate was 3 870 mm^2 (one half of 76 × 102 mm plate) in both cases, and 47 teeth were modeled in each half of the joint. However, the specific orientation of teeth rows (30 and 60° to the joint main axis, respectively) added complexity to the model. To simplify the model, we disregarded the exact geometric layout of the spring elements, and distributed them in a simpler fashion, copying the teeth layout of models T0 and TP90. However, the overall shape of the plate, the number of teeth (spring elements), and teeth density were kept the same. Also, the load-slip properties of the spring elements were still defined in the directions of the original plate main axes (from R30 and R60 models). R30 and R60 were the only joint configurations investigated in this section.

Lumping the Teeth Properties. Instead of three spring elements describing the behavior of each tooth separately in the model, a number of teeth were represented by one group of three spring elements ("super nodes"). These elements were assigned the load-slip characteristics for a group of teeth. This was implemented by multiplying the load side of the L-D curve by the number of teeth involved in that particular group. T0 and B0 were the only joint configurations examined in this study. Two different configurations of super nodes were investigated—four super nodes located at the corners of half the plate, and four super nodes each placed at one quarter distance (of half plate length and half plate width) from the corners of half the plate.

Results and Discussion

Validation of Four Basic Tensile Models and Sensitivity Analysis

Validation of Four Basic Tensile Models. The four basic models (T0, T90, TP0, and TP90) were loaded in the same direction as one of the original tests that yielded their properties. Thus, the model results were expected to match the corresponding test results, since, in essence, the models were "calibrated" with the experimental data. And indeed, the results matched well over the entire L-D path for all four basic tensile models.

Sensitivity Analysis. *Wood Stiffness.* The stiffness properties assigned to wood elements (MOEs) were reduced to one half of their original values, and model results were compared to the original T0 results. The overall joint stiffness measured at the plate was not influenced with this variation of the assigned wood member stiffness. However, it is important to note that the per-tooth load-slip properties (obtained from testing) partially depend on the actual stiffness of the wood fiber (along with the specific gravity, etc.). Therefore, the stiffness is partially incorporated in the model through the wood-plate contact elements. Also, the actual joint displacements for all tests (and for all models) were observed near the plate and relative to the plane between the two members, therefore the overall wood elongation does not significantly affect the deflection at the observed point.

Steel Stiffness. A similar comparison was done with steel stiffness reduced to half of its original value. The assigned steel stiffness only slightly influenced the overall stiffness of the modeled joint. This phenomenon may be explained by the fact that for joints with the investigated plate size, the stiffness and failure mode are governed by the plate-wood interface behavior, which is included in the model through the per-tooth load-slip curves. For joints with larger plates, however, where the capacity of teeth "grip" exceeds the capacity of the plate strength, the steel stiffness and strength may become the determining factor governing the overall behavior of the joints.

In-Plane Per-Tooth Parameters. Furthermore, a comparison was made between two joint models where the in-plane per-tooth load-slip parameters were varied. Figure 6 shows the comparison between the overall stiffness of the T0 joint model, and the same model, but with the stiffness in the x direction assigned based on the x direction stiffness from the T90 test. There is a significant difference between the two. Therefore, it was concluded that the behavior of joint models loaded in tension is governed by the in-plane load-slip parameters assigned at the per-tooth level.

Z-Direction Stiffness. Finally, it was necessary to validate the assumption that the assigned stiffness in the z direction does not affect the behavior of joint models when loaded in the plane of the joint. After comparing the T0 model results with a model for which the stiffness in the z direction was reduced to half of its original value, it was shown that the overall L-D behavior of the joint was not affected. Therefore, it was concluded that the same average per-tooth L-D curve in the z direction should be assigned to all the rest of the joint models.

It is important to emphasize that the results from the sensitivity analysis apply only to joint models with the

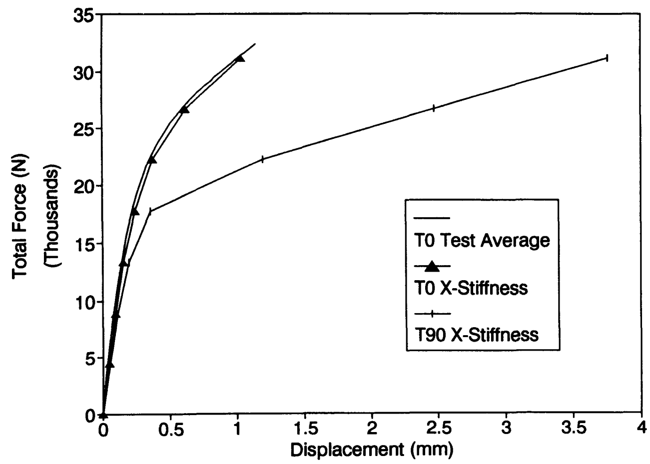

Figure 6–Comparison of T0 models with different spring-element x-direction stiffnesses.

investigated plate size (small), and without further investigation they could not be fully accepted and universally applied to all MPC joint models.

Model Validation

R Models. The loads imposed on R30 and R60 models (and tested joints) were not coincident with the direction of either plate axis, so the results were not simply "calibrated", as was the case in previous models (T0, T90, TP0, and TP90). Figures 7a and 7b show the comparison between the test and model results for tests R30 and R60. A minor difference between the curve slopes for both L-D curves is noticeable. However, the results for both models fall within the region covered by the original L-D curves for the corresponding tests.

B Models. The comparison between the L-D curves obtained from testing and the model, for four bending tests, is shown in figures 8a, 8b, 8c, and 8d. The results match throughout the entire L-D range. The model L-D curves fall within the scatter of the original data L-D curves for corresponding tests. The wood-to-wood contact elements are a very important feature of the model. For comparison purposes, several joint models loaded in bending were developed without wood-to-wood contact elements, and the results were compared, as shown in figure 9. The model without contact elements proved to be too flexible in bending. The models with contact elements predict the behavior well, while the ones without contact elements do not. This demonstrates that wood-to-wood contact is a significant feature determining the overall behavior of MPC joints where wood members come in contact.

Model Simplifications

Plate Slots. The comparison between the L-D results of the two model approaches (slots and no slots) for the same joint (T0) showed that practically no difference existed between the two. The stiffness of joints with the investigated plate sizes is mostly influenced by the plate-wood interaction. For joints with larger plates, however, the plate properties may become the determining factor governing the stiffness and failure mode of the joints, and plate slots may need to be included in the model.

Also, in omitting the slots from the model (therefore eliminating stress concentrations and increasing the overall cross-section of the plate), a compromise was obviously made with respect to the stresses created in the model plate.

Teeth Layout. There was no noticeable difference in the L-D curves when the results from the original R30 and R60 models and the results from the modified R models (based on the teeth geometries of T0 and TP90 models) were compared. A comparison for model configurations loaded in bending (B30 and B60 vs. modified B models based on the geometries of T0 and TP90 models) showed that the results were again very similar, and the same conclusions were drawn: the "micro-distribution" of spring elements, given the same number and density of "teeth", does not play a significant role in the overall displacement of MPC joints.

Lumping the Teeth Properties. The results from joint models with lumped teeth properties, loaded in tension and bending, are shown in figures 10a and 10b, respectively. For the investigated tensile joint model, both altered-teeth layout configurations proved to be less stiff than the original one. However, the results for the layout where super nodes were more uniformly distributed over the area of the plate showed a better match with experimental data. In the bending model, the results showed that the model became stiffer as the super nodes were moved farther from the geometric center of the plate, which was to be expected because of increased polar moment about the geometric center of the plate.

It is a matter for future studies to search for the optimum number and location of super nodes that would model the MPC joint behavior most successfully. However, even the preliminary results obtained from these two simplified super node layouts show a potential value. It is conceivable to speculate that such simplifications at the joint level, once resolved, might be successfully used in overall truss analyses, where one is mostly concerned with global truss displacements and member force distribution.

Conclusions

The finite-element model developed in this study is capable of accounting for a large number of factors influencing the joint performance while in service. The models of simple MPC joints with various plate-grain

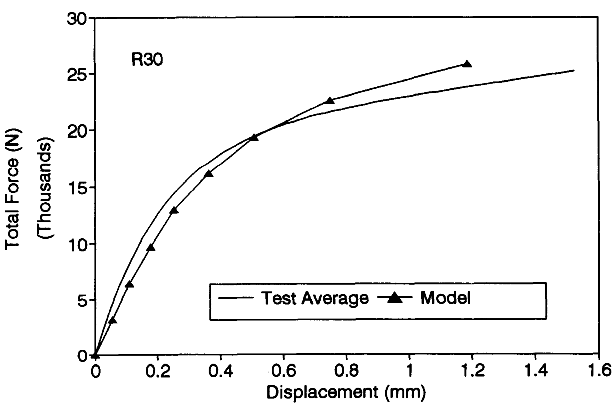

(a)

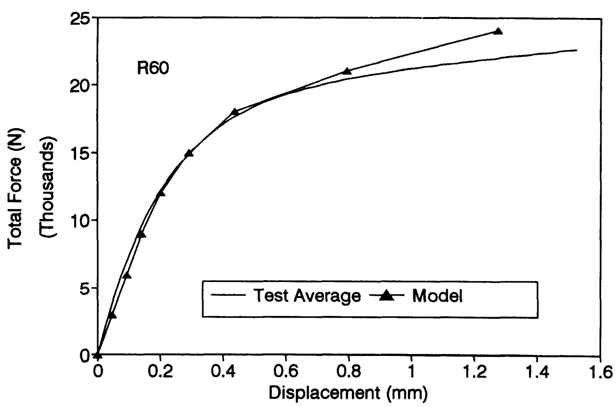

(b)

Figure 7–R models (tensile force parallel to grain, plate-grain orientation varied): comparison with test results. (a) R30 model (plate-grain orientation at 30°) and (b) R60 model (plate-grain orientation at 60°).

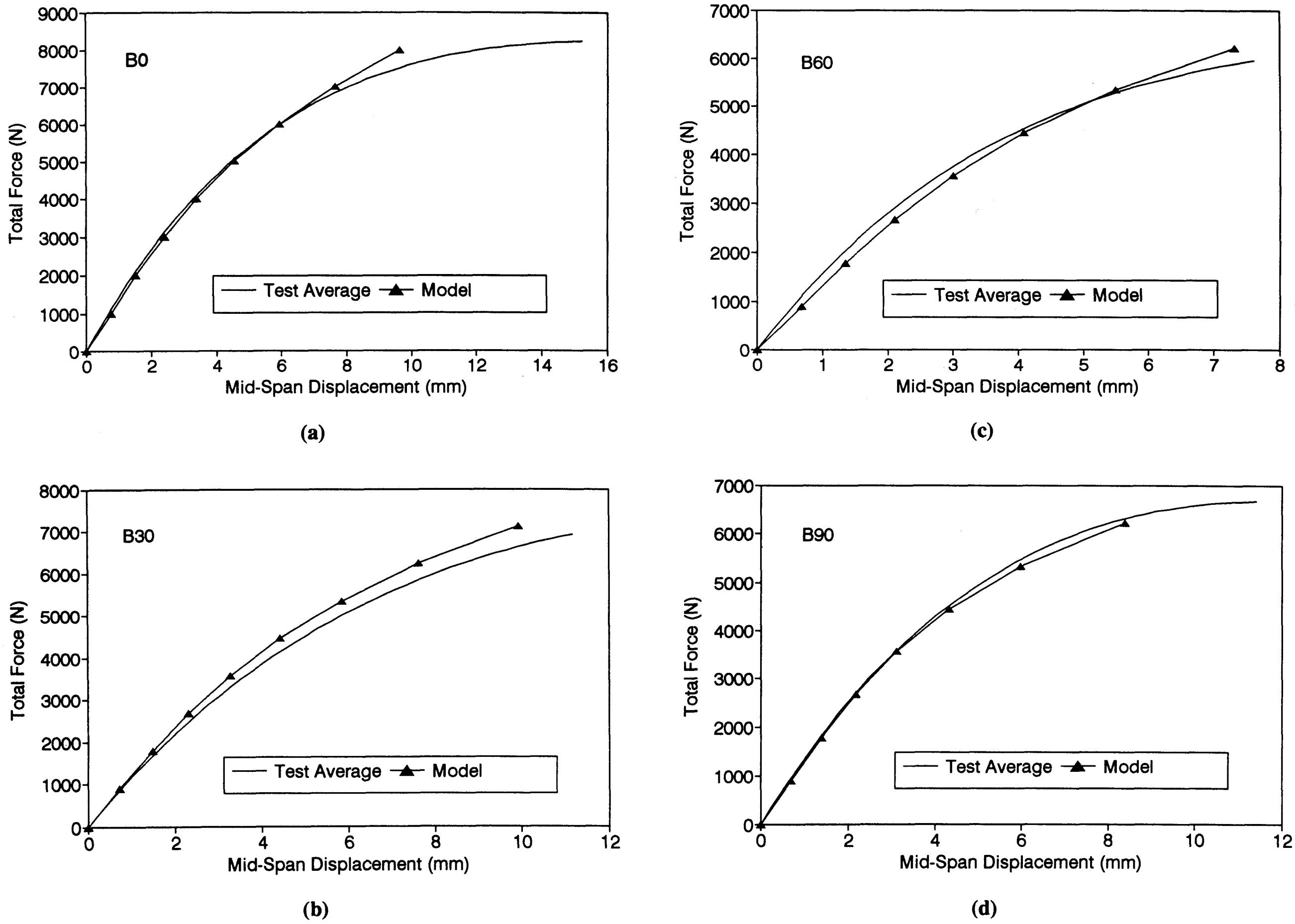

Figure 8–B models (models loaded in bending, plate-grain orientation varied): comparison with test results. (a) B0 model (plate parallel to grain), (b) B30 model (plate-grain orientation at 30°), (c) B60 model (plate-grain orientation at 60°), and (d) B90 model (plate perpendicular to grain).

orientations exposed to different loading conditions demonstrate the plausible applicability of the method to more complex, actual joint configurations.

Also, even though not directly investigated in this study, this model, by including steel plate properties, is potentially capable of adequately representing MPC joints with larger plate-covered areas, where the overall behavior is governed by the steel plate properties, and not by the wood-plate interaction.

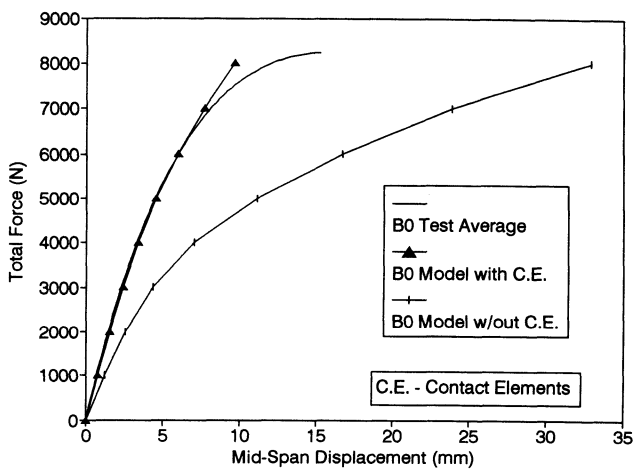

Figure 9–B0 model vs. B0 model without contact elements.

Finally, if a reliable method for determining the optimal distribution and number of "super nodes" can be found so that a simpler model can accurately represent the overall stiffness of the connections, the modeling approach illustrated here could eventually become feasible for truss analysis and design.

With the advancement of computer technology, where various programs are now integrating graphic design software with specialized analytical tools, the realization of the ultimate goal of this study might be closer than expected. The users will be able to create three-dimensional truss models through an interactive computer-screen interface, resulting in a tremendous simplification of the method.

ACKNOWLEDGMENTS. The authors gratefully acknowledge the assistance of Alpine Engineered Products, Inc., for donating the metal plates for testing, and especially Stuart Lewis, the Research and Development Manager, for assistance throughout the project, and to Frank Lumber Co., Mill City, Oregon, for donating lumber.

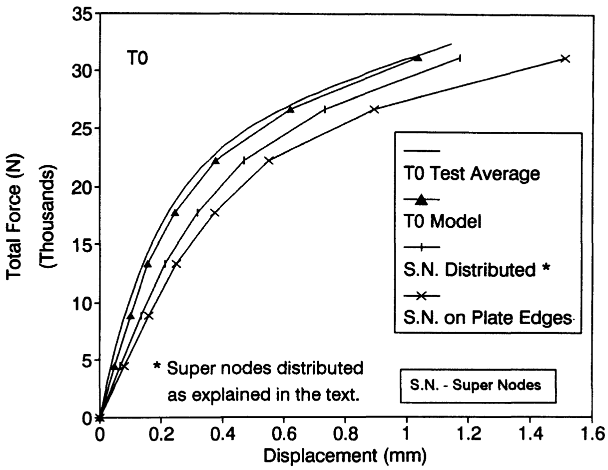

(a)

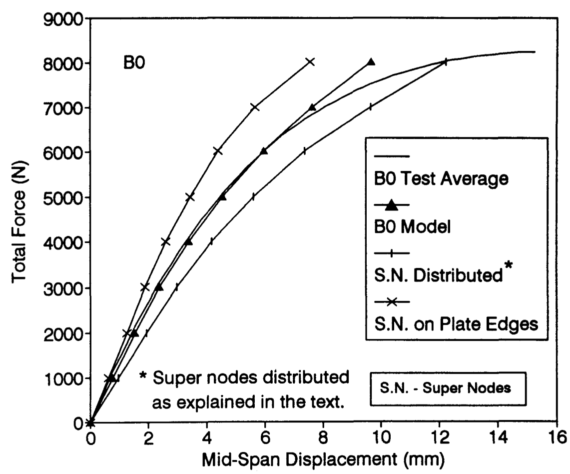

(b)

Figure 10–(a) T0 model vs. T0 model with different super node layouts, and (b) B0 model vs. B0 model with different super node layouts.

References

ANSYS. 1992. *ANSYS User Manual for Revision 5.0.* Houston, Pa.: Swanson Analysis System, Inc.

Canadian Standards Association (CSA). 1980. CSA Standard S 347-M1980. Method of test for evaluation of truss plates used in lumber joints. Rexdale, Ontario, Canada.

Cramer, S. M., D. Shrestha and W. B. Fohrell. 1990. Theoretical consideration of metal-plate-connected wood-splice joints. *J. of Structural Eng.* 116(12):3458- 3474.

Cramer, S. M., D. Shrestha and P. V. Mtenga. 1993. Computation of member forces in metal plate connected wood trusses. *Structural Eng. Review* 5(3):209-217.

Crovella, P. L. and K. G. Gebremedhin. 1990. Analysis of light frame wood truss tension joint stiffness. *Forest Products J.* 40(4):41-47.

Eshbach, O. V. 1990. *Handbook of Engineering Fundamentals*, 4th Ed. New York: Wiley Interscience Publication.

Forest Products Laboratory 1987. *Wood Handbook: Wood as an Engineering Material.* Agric. Handbook 72. Washington D.C.: USDA.

Foschi, R. O 1979. Truss plate modeling in the analysis of trusses. In *Proc. of Metal Plate Wood Truss Conf.* Madison, Wis.: Forest Products Soc.

McCarthy, M. and R. W. Wolfe. 1987. Assessment of truss plate performance model applied to southern pine truss joints. Research Paper FPL-RP-483. Madison, Wis.: USDA-Forest Service, Forest Products Laboratory.

Reynolds, G. M. 1988. Analysis and testing of toothed metal plate wood truss connections. M.S. thesis, Michigan Technological Univ., Houghton, Mich.

Triche, M. H. and S. K. Suddarth. 1988. Advanced design of metal plate connector joints. *Forest Products J.* 38(9):7-12.

Vatovec, M. 1996. Analytical and experimental investigation of the behavior of metal-plate-connected wood truss joints. Ph.D. thesis, Oregon State Univ., Corvallis.